Fast auroral snapshot satellite observations of very low frequency saucers

R. E. Ergun
The Department of Astrophysical and Planetary Sciences and the Laboratory for Atmospheric and Space Physics, University of Colorado, Boulder, Colorado 80303

C. W. Carlson and J. P. McFadden
Space Sciences Laboratory, University of California, Berkeley, California 94720

R. J. Strangeway
Institute for Geophysical and Planetary Physics, University of California, Los Angeles, California 90055

M. V. Goldman and D. L. Newman
The Department of Physics and the Center for Integrated Plasma Studies, University of Colorado, Boulder, Colorado 80303

(Received 13 May 2002; accepted 24 October 2002)

Wave and charged particle observations of quasielectrostatic whistler emissions known as ''VLF saucers'' (very low frequency, or kilohertz radio range) from the Fast Auroral SnapshoT (FAST) satellite demonstrate that the majority ($\sim$85%) of VLF saucer emissions are generated on flux tubes that carry antiearthward, energetic ($>$10 eV) electrons in the downward current region of the aurora. In most cases, the VLF saucers are nested, that is, they have two or more clearly discernible ''arms'' that indicate several distinct source regions at differing altitudes. These observations verify previous interpretations that the individual source regions are highly localized both in latitude and altitude. In some cases, the individual source regions are localized in three dimensions. An important new finding is that the FAST satellite frequently detects solitary structures identified as electron phase-space holes at the vertex of VLF saucers. Electron phase-space holes were identified in $\sim$79% of the VLF saucer events in the downward current region. This finding implies either a common energy source or a direct association between the two phenomena. Furthermore, the observations now show a direct association with the VLF saucer source flux tube and diverging dc electric field structures. An interpretation is put forth that the VLF saucer source region is in or near parallel electric fields in the downward current region of the aurora. © *2003 American Institute of Physics.*
[DOI: 10.1063/1.1530160]

I. INTRODUCTION

FAST satellite observations have established that the downward current region is an active part of the aurora and must be considered an essential component of magnetospheric-ionospheric coupling.[1] There is compelling evidence that quasistatic, parallel electric fields are responsible for accelerating electron fluxes antiearthward to near keV energies.[2–5] The electron distributions that emerge from the parallel electric fields most likely are highly unstable and are seen to generate a variety of wave modes and plasma structures including VLF saucers.[6] These waves and plasma structures, in turn, strongly modify and rapidly stabilize the electron distributions and energize the ambient ion population to the extent that they can overcome the parallel electric fields and escape resulting in strong ion outflow. The focus of this article is to expand upon the findings from the FAST satellite on VLF saucers reported by Ergun *et al.*[6]

VLF saucers are one of the most intense wave emissions in the downward current region. They are among the first radio-wave features observed in the auroral zone[7,8] and have been established as a common characteristic of that region.[9] The phenomenon is characterized by a V-shaped or saucer-shaped appearance in a time-frequency-power spectrogram of wave electric fields in the kilohertz frequency range. Such V-shaped structures are seen over a range of time (or distance) scales ranging from less than a second ($<$5 km) to hundreds of seconds ($>$1000 km), prompting several naming conventions which include ''short saucers,'' ''auroral V emissions,'' and ''V-shaped VLF hiss.'' We concentrate on a class of V-shaped emissions observed by low altitude ($<1R_E$) satellites that are intense ($>10^{-9}$ $V^2\,m^{-2}\,Hz^{-1}$), in the frequency band of $\sim$1 kHz to 16 kHz, and commonly referred to as VLF saucers.

The saucer- or V-shaped appearance was shown to be consistent with propagation properties of quasielectrostatic whistler waves.[10,11] The lowest frequency emissions are near the lower hybrid frequency and have a group velocity nearly parallel to the ambient magnetic field ($\boldsymbol{B}$). Higher frequency quasielectrostatic whistler emissions have an oblique group velocity; the higher the frequency, the larger the angle from $\boldsymbol{B}$. Thus, as a satellite passes over a continuous, stationary source region it detects the higher frequencies far away from flux tube of the source and the lowest frequencies as it passes over the flux tube of the source.

One of the most intriguing features of VLF saucers is the small physical size of the source regions that are inferred from the observations.[9] The ISIS 2 satellite included an active sounder which measured the ionospheric density profile.

Using this measured density profile, the source region location and size could be determined via ray tracing. The source regions were found to be as small as 0.5 km in latitude and less than 10 km in altitude. It is possible, however, that the source of VLF saucers may have a larger extent in longitude.[12]

A statistical study of the occurrence of VLF saucers was made from the ISIS 2 data base.[9] Under that study, VLF saucers were not found below 1000 km in altitude; the occurrence frequency increased with increasing altitude up to ~3000 km, the limit of the study. Saucers were observed primarily at magnetic local times near midnight. Later, the S3-3 satellite[13] and the Viking satellite[14] observed saucers up to 13 500 km in altitude (the apogee of Viking) and at all local times. Interestingly, studies from the S3-3 satellite demonstrated a correlation between dc electric field structures and VLF saucers,[13] but no distinction was made between converging or diverging structures (upward or downward current region).

The energy source of VLF saucers was an enigma for quite some time. Early satellite observations suggested that the source regions are on the equatorward or poleward boundaries of the visible (i.e., upward current region) auroral zone, implying that they are in the downward current region. However, no clear signature in the electron or ion distributions was detected at that time.[15] James[9] postulated an instability from cold (<5 eV), dense, up-going ionospheric electrons carrying the downward or ''return'' current in the auroral zone impinging upon a warm magnetospheric population. Using linear growth rate calculations, he demonstrated that a strong enough instability was plausible. The cold ionosphere electrons were thought to be too low in energy to have been detected by the satellite instruments at the time.

Over a decade later, the Viking satellite detected up-going electrons associated with VLF saucers in several events and verified that the majority of events were in the downward current region.[14] In one of these events, a sharp increase the flux of ~100 eV up-going electrons was observed at the vertex (the point of lowest-frequency emissions) of a VLF saucer. As it crossed the source flux tube, the satellite observed intense broadband emissions from dc up to the plasma frequency.

The recent uncovering of energetic (up to several keV) electron fluxes accelerated by parallel electric fields carrying the downward current in the auroral zone[2,3] reveals a conspicuous candidate for the VLF saucer energy source. Inspection of the wave and particle observations from the FAST satellite indicates that a large majority of the VLF saucer sources were on flux tubes carrying intense, up-going energetic electron fluxes. These fluxes avoided detection by previous satellites because they are restricted to a narrow latitude and have a very narrow range in pitch angles. FAST observations, with continuous monitoring of the field-aligned electrons, now provide conclusive evidence that energetic, up-going electrons are, in fact, the energy source of VLF saucers.

Several new features of VLF saucers emerge in high time-resolution wave observations. VLF saucers often appear to have multiple ''arms.'' Each arm originates from a distinct source region that appears to be confined in longitude as well as latitude and altitude, in other words, a ''point'' source. Thus, multiple arms indicate many individual source regions dispersed in longitude and altitude rather than a single source extended in longitude as postulated earlier.[12]

Further examination of the VLF saucer wave spectra verifies that the intense broadband bursts detected by Viking[14] are a frequent phenomenon at the vertex (or source flux tube) of VLF saucers. FAST high-resolution waveform observations reveal that these broadband bursts represent a series of solitary structures that have been identified as electron phase-space holes.[6,16,17] In the downward current region, electron phase-space holes are traveling antiearthward on the same flux tubes as the VLF saucer source region. A small survey of events indicates that the electron-phase space holes are observed regardless of the distance from the apparent source region. Since the longevity of electron phase-space holes is not well known, these observations, at this time, cannot be unequivocally interpreted. It is possible that the electron holes are co-generated with the VLF saucer emissions. However, the fact that electron holes are often observed with no discernible VLF saucer emissions complicates this interpretation.

FAST observations also show a correlation between VLF saucers and diverging dc electric field structures. This result is in agreement with earlier studies[13] in which no distinction was made between converging or diverging structures but now can be re-interpreted in the light of the recent finding of parallel electric fields in the downward current region.[2,3] We put forth a hypothesis that the VLF saucer source region may be in or near the parallel electric fields. Under this hypothesis, the small size of the VLF saucer source region suggest that the parallel electric fields in the downward current region are confined to a thin layer in altitude.

II. CHARACTERISTICS OF VLF SAUCERS

The V-shaped appearance in a time-frequency-power spectrogram is thought to come from propagation characteristics of quasielectrostatic whistler waves.[9–15] A linear growth and propagation analysis suggested that electron acoustic mode also could produce a similar spectral signature.[18] The electron acoustic mode, however, requires two electrons populations with a temperature ratio $T_{\mathrm{hot}}/T_{\mathrm{cold}} \gg 1$. It is often difficult to determine if this condition is met from the measured electron distributions, particularly near the source flux tubes since electrons with energies below ~5 eV are not measured accurately. The emissions at the source flux tube, however, sometimes show a magnetic signature indicating the presence of whistler waves.[15] Furthermore, we find many cases away from the source flux tube in which the measured electron distributions do not support propagation of the electron acoustic mode. VLF saucer emissions are often seen in a plasma environment with no detectable hot electron population[14] where the electron acoustic mode is strongly damped. Even though we cannot rule out the electron acoustic mode in all cases, we presume that the VLF saucer emissions are from whistler waves in this paper.

Under the cold fluid approximation, the wave vector di-

rection (θ, the angle from the magnetic field, $\boldsymbol{B}$) depends upon the wave frequency (ω):

$$\frac{k_\perp^2}{k_\parallel^2} = \tan^2\theta = \frac{-\left(1-\frac{\omega_{pe}^2}{\omega^2}-\frac{\omega_{pi}^2}{\omega^2}\right)}{\left(1-\frac{\omega_{pe}^2}{\omega^2-\omega_{ce}^2}-\frac{\omega_{pi}^2}{\omega^2-\omega_{ci}^2}\right)}, \tag{1}$$

where ω_{pe} (ω_{pi}) and ω_{ce} (ω_{ci}) are the electron (ion) plasma and cyclotron frequencies. The above equation is for a single ion species and easily can be generalized for multiple species. In many cases, a simple approximation can be used:

$$\omega \cong \omega_{pe}\cos\theta \quad (\omega_{ce} \gg \omega_{pe} \quad \text{and} \quad \omega \gg \omega_{pi}, \omega_{ci}). \tag{2}$$

Since the relationship between the wave frequency and wave vector ($\boldsymbol{k}$) only depends on the direction of $\boldsymbol{k}$, it follows that the group velocity ($\boldsymbol{v}_g = d\omega/d\boldsymbol{k}$) is perpendicular to $\boldsymbol{k}$ and can be expressed as

$$\sin\theta_{\text{group}} \cong \frac{\omega}{\omega_{pe}} \quad \omega_{ce} \gg \omega_{pe} \quad \text{and} \quad \omega \gg \omega_{pi}, \omega_{ci}. \tag{3}$$

A more precise expression can be derived from Eq. (1).

The shape of a VLF saucer in a time-frequency-power spectrogram depends on the distance from the source and the satellite velocity as well as the magnetic field, the plasma density, and the plasma composition over the propagation path of the whistler waves. It is often difficult to accurately calculate the distance to the source, particularly for remote sources, since a plasma density model and detailed ray tracing is required.[9] The altitude of the source region for nearby sources, however, can be estimated by assuming a homogenous plasma density and plasma composition at the values observed by the passing satellite. Under the above approximation and the approximations used in Eq. (2), the distance from the source can be expressed as

$$d \cong \frac{v_{\text{sat}}\omega_{pe}}{\left.\frac{d\omega}{dt}\right|_{\omega_0}} \quad (\omega_{ce} \gg \omega_{pe} \quad \text{and} \quad \omega \gg \omega_{pi}, \omega_{ci}), \tag{4}$$

where v_{sat} is the satellite velocity and $d\omega/dt$ is the slope of the saucer boundary in a time-frequency-power spectrogram. Equation (4) is an approximate solution. In this work, fits using the full cold-fluid dispersion relation, Eq. (1), also are used to determine the distances to the sources.

Figure 1 demonstrates how wave spectra vary with source location and size. The traces are examples of ideal power-frequency-distance (or time) spectrograms from point source locations. The solid trace is from a point source 100 km in altitude below the spacecraft as measured at the vertex. The plasma conditions in Fig. 1 assume an electron density n_e of 20 cm^{-3}, a constant magnetic field ($\boldsymbol{B}$) at 10 000 nT, and a homogeneous H^+ plasma. The trace forms a V in the spectrogram with a low-frequency cutoff at the lower hybrid frequency. The dotted trace displays the expected wave spectrogram from a point source 200 km below the spacecraft. The V is less steep but otherwise shows the same low-frequency cutoff. Comparing these two traces demonstrates how the source size can be determined. The extent of the source in altitude determines the bandwidth of the spectra at the higher frequencies (far from the vertex in horizontal distance along the spacecraft path), but does not dramatically change the spectra at the vertex. Thus, one determines the location and extent in altitude of the source region by examining spectra at higher frequencies far from the saucer vertex.

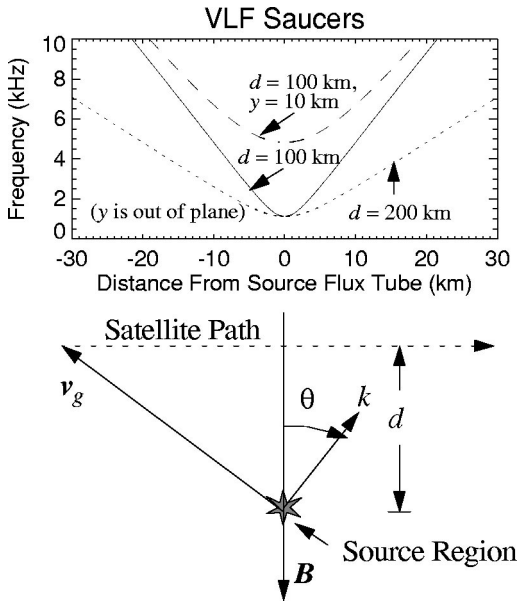

FIG. 1. The top box shows the relation between the frequency and horizontal distance between the satellite and the source flux tube. The solid trace is from a point source in a homogeneous H^+ plasma (20 cm^{-3}) and constant magnetic field (10 000 nT) as measured by a satellite 100 km above the source region. The dotted trace is from a point source 200 km below the satellite, and the dashed trace is from a point source 100 km below the satellite and 10 km out of the plane defined by the satellites' path and the magnetic field. The "V-" or "saucer-" shaped time-frequency-power spectrograms of electric field waves comes from the propagation characteristics of quasielectrostatic whistler waves. The shape of the saucer depends on the magnetic field, plasma density, the velocity of the satellite, and the relative location of the source.

The dashed trace in Fig. 1 illustrates the effect of an out-of-plane displacement of the source region. The source is 100 km below the spacecraft but 10 km out of the plane defined by the spacecraft path and magnetic field. In the case of an auroral satellite traveling in the North–South direction, the displacement would be in longitude. When compared to the solid trace, the dashed trace shows the greatest change near the vertex. It has a cutoff at a significantly higher frequency because the minimum propagation angle is nonzero. Farther from the source, that is, in horizontal distance along the spacecraft track, the effect of the out-of-plane displacement of the source is less pronounced. Thus, one determines the longitudinal position and size by examining spectra near the saucer vertex. Unfortunately, broadband emissions from electron phase-space holes at the vertex often complicate such an analysis.

The finite size of a source in the direction along the spacecraft path increases the bandwidth of the saucer spectra. Saucer spectrograms often have narrow banded tone that falls (or rises) as the satellite moves towards (or away) from the source flux tube. This characteristic indicates a small source region in altitude and latitude in the case that the

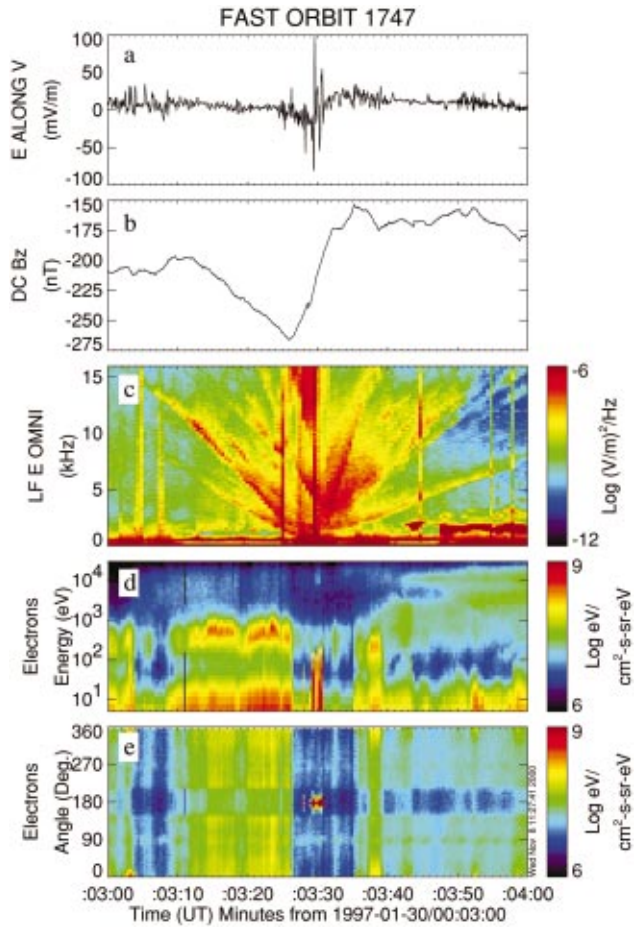

FIG. 2. (Color) (a) The perpendicular electric field in the spin plane and nearly along the spacecraft path (mostly North). The negative electric field signal starting at ~00:03:25 UT followed by a positive signal at ~00:03:30 UT corresponds to a diverging electric field structure indicative of a downward parallel electric field. (b) ΔB along the spacecraft spin axis (mostly West) and normal to the spacecraft velocity. A negative slope indicates upward current; a positive slope indicates downward current. (c) The electric field spectral power density summed over all directions. A VLF saucer with multiple arms is apparent. (d) Electron differential energy flux versus energy, and (e) versus pitch angle. At the vertex of the VLF saucer, intense, low-energy, up-going (180°) electron fluxes dominate the spectra.

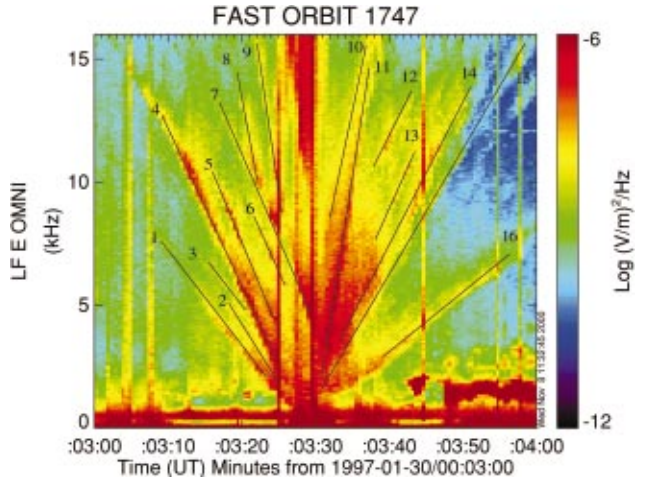

FIG. 3. (Color) An expanded view of Fig. 2(c) shows at least 16 distinct ''arms'' indicating eight or more three-dimensionally confined source regions. Each of the individual source regions extends less than 10 km altitude and latitude, and less than 20 km in longitude. The source regions range from ~100 km (closest) to ~700 km (farthest) below the spacecraft in altitude, have vertices from 00:03:25 UT to 00:03:35 UT (~50 km in latitude), and have longitudinal displacements (direction cannot be determined) up to ~50 km.

satellite is traveling North or South.[9] We present high time resolution data that have signatures that imply a source region that is confined in three dimensions.

Since the FAST satellite does not have an active sounder, the density models are less precise than those used on ISIS 2, and thus the estimations of the source distance and sizes are less precise. The O^+/H^+ ratio is determined at 30 s intervals on FAST.[1] In this article, the estimates of distances assume a constant density along the propagation path and a stationary source.

III. OBSERVATIONS

We begin with VLF saucer observations from the FAST satellite. The instruments are described elsewhere[1,19–21] so we include only minimal details here. Figure 2 displays 60 s of wave and particle observations during a large-scale VLF saucer event in a near-dawn crossing of the Northern auroral zone at ~3300 km in altitude. The spacecraft was traveling approximately from North to South, so the horizontal axis can be interpreted as North–South distance as well as time. The spacecraft velocity was ~5 km/s.

The top panel of Fig. 2 displays the dc electric field signal along the path of the spacecraft (nearly Southward) and perpendicular to the ambient magnetic field. This direction is defined as the $(\boldsymbol{v}_{sc}\times\boldsymbol{B})\times\boldsymbol{B}$ direction where $\boldsymbol{v}_{sc}$ is the spacecraft velocity and $\boldsymbol{B}$ is the ambient magnetic field. The signal is negative beginning at ~00:03:25 UT and then shifts to positive at ~00:03:30 UT. This signature is that of a diverging electric field structure which implies a downward parallel electric field is on the flux tube of the spacecraft at a lower altitude.[3] Figure 2(b) displays the mostly East–West ($\boldsymbol{v}_{sc}\times\boldsymbol{B}$ direction) perturbation magnetic field signal ($\Delta\boldsymbol{B}$); a model magnetic field has been subtracted. The slope of the magnetic field signal indicates a current, assuming a sheet-like structure. A negative slope implies an upward current and a positive slope implies a downward current. The region of interest (~00:03:25 UT to ~00:03:35 UT) has a strong positive slope indicating a downward current of ~2 μA/m^2.

Figure 2(c) displays the electric field spectral power density in the 0–16 kHz range. The dominant feature is a complex, multiple-arm, VLF saucer with the vertex at ~00:03:30 UT. The vertical features in the plot (e.g. ~00:03:25 UT, 00:03:29.5 UT, 00:03:45.5 UT) are bursts of broadband electrostatic noise. Figure 2(d) displays the electron differential energy flux (color) as a function of energy (vertical axis) and Fig. 2(e) displays the electron differential energy flux as a function of pitch angle. Earthward traveling electrons are at 0° and 360° and antiearthward electrons are at 180°. During most of the 60 s period, the electron fluxes were traveling predominantly earthward. At the apex of the VLF saucer, however, intense fluxes of highly field-aligned, ~100 eV, electrons were traveling antiearthward. Figure 2 displays a clear example in which the VLF saucer source is associated

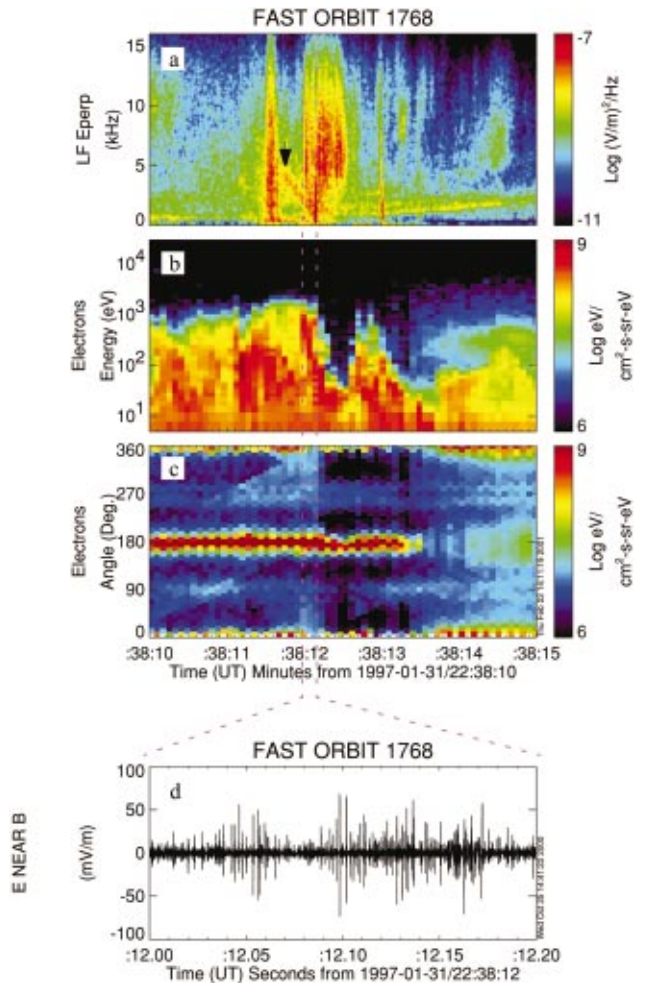

FIG. 4. (Color) A VLF saucer with a nearby source region. (a) The electric field spectral power density summed over all directions. The short arm marked on the plot with an arrow has a source region ~30 km from the spacecraft. The resolved, narrow bandwidth indicates a source region size of less than 1 km in altitude and less than 0.3 km in latitude. (b) Electron differential energy flux versus energy, and (c) versus pitch angle. Intense, low-energy, up-going (180°) electron fluxes dominate from the beginning of the plot until ~22:38:13 UT. (d) An expanded view (0.2 s) of the parallel waveform (1 kHz–16 kHz band). The above event was at 3350 km altitude, 74.8 invariant latitude, and 6:00 a.m. magnetic local time.

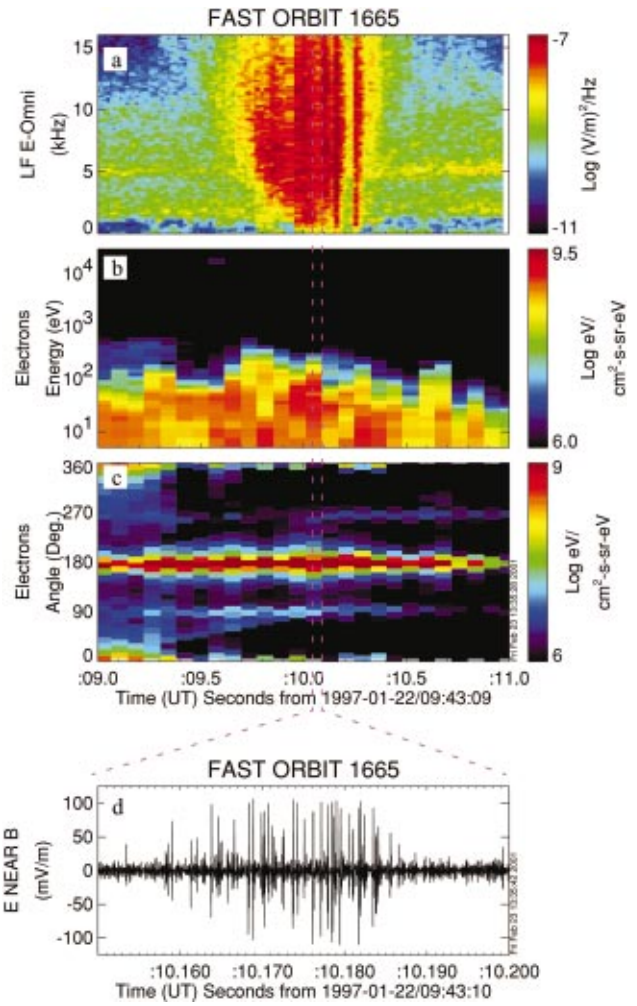

FIG. 5. (Color) A VLF saucer with a nearby source region. (a) The electric field spectral power density summed over all directions. (b) Electron differential energy flux versus energy, and (c) versus pitch angle. Intense, low-energy, up-going (180°) electron fluxes dominate throughout the plot. (d) An expanded view (50 ms) of the parallel waveform (1 kHz–16 kHz band). The above event was at 4158 km altitude, 76.1 invariant latitude, and 22:84 a.m. magnetic local time.

with antiearthward electron fluxes that were accelerated by a parallel electric field.

A close examination of the electric field spectral power density reveals multiple sources (Fig. 3). There appear to be at least 16 distinct arms in the VLF saucer, indicating at least eight distinct source regions. An unambiguous pairing of the arms cannot be made without an accurate density profile, particularly since the broadband bursts obscure the VLF saucer arms at the vertex.

The slopes and bandwidths of the arms provides information on the individual source sizes and locations. The narrow bandwidth (~40 Hz) of each of the arms far from the source indicates that each of the sources is limited to at most ~10 km extent in altitude and in latitude. The slope of the arm labeled 16, for example, indicates a source distance of ~700 km from the spacecraft at the vertex, given a constant plasma density along over the propagation path. The closest source region, arm 11, is ~100 km from the spacecraft. The vertices of the arms map from 00:03:25 UT to 00:03:35 UT, during which time the spacecraft traversed ~50 km, so the individual sources may be dispersed over this region in latitude. The size of the nearest sources are less than ~2 km in latitude.

The bandwidth of the arms increases near the vertex (at lower frequencies), indicating a finite longitudinal size. Because of the multiple arms and the broadband electrostatic noise (vertical features), the longitudinal size cannot be determined for all of the arms. Arms 1, 4, and 16, however, suggest a longitudinal size less than ~20 km for their respective source regions. Longitudinal displacements of up to 50 km are also possible.

The above observations support many of the conclusions drawn from the ISIS 2 data[9] and Viking measurements.[14] The energy source appears to be from antiearthward electron beams. The source regions are confined in both latitude and altitude to less than ~10 km. The FAST observations, how-

ever, further suggest that at least some of the individual VLF sources are also confined in longitude and that the electron beams are accelerated by a parallel electric field.

The most accurate estimates of the source size can be obtained from the nearest sources. Figure 4 displays a small-scale VLF saucer that has a nearby source. The time axis is greatly magnified from that of Figs. 2 and 3, covering only 5 seconds, during which time the satellite traversed ~25 km. The top panel displays the electric field spectral power density. Figures 4(b) and 4(c) display the electron differential energy flux in the same fashion as in Fig. 2. The small arm with a vertex at ~22:38:12.15 UT, marked with an arrow on Fig. 4(a), has a slope consistent with a source ~30 km from the spacecraft, yet displays a narrow (~200 Hz full width at half maximum at 4 kHz) bandwidth. The right-hand side of the event displays a much broader bandwidth. If the source is stationary, the source size (Δd) scales with the bandwidth and the distance from the source,

$$\frac{\Delta d}{d} = \frac{\Delta \omega}{\omega \cos^2 \theta} \tag{5}$$

the marked arm suggests a source region of roughly 1 km in altitude and less than 0.3 km in latitude. This event represents the smallest source region found in the FAST data set thus far. Figure 4(d) is discussed below.

Figure 5 shows another nearby source with the same layout as in Fig. 4. The time scale in this event is only 2 seconds during which time the satellite traversed ~10 km. The event, if interpreted as a nearby VLF saucer, had a source less than 10 km from the spacecraft at the vertex. The broad bandwidth indicates that the source size is less than ~0.5 km in latitude but could be up to ~10 km in altitude. These estimates match those put forth by James.[9]

The lower panels (d) of Figs. 4 and 5 illustrate the nature of the broadband electrostatic noise often seen at the vertex of VLF saucers. The electric field waveforms parallel to ***B*** contain a series of bipolar spikes similar to those that were previously reported.[16,17] These structures have been identified as nonlinear BGK solution to the Vlasov–Poisson equations known as electron phase-space holes. Electron phase-space holes were found to be traveling at roughly the electron drift speed antiearthward along ***B***. Thus, the structures are on the source flux tube of the VLF saucers, emerging from the direction of the source. These findings suggest a connection between the two phenomena.

Once the distance to the source and the source size have been estimated, the intensity of the emissions in the source region can be approximated. The arm labeled 4 in Fig. 3, for example, has emissions of $\sim 10^{-6}$ $(\mathrm{V/m})^2/\mathrm{Hz}$ from a source ~300 km away. Assuming a source size of 10 km and a constant plasma density along the source path, the electric field amplitude at the source would be >100 mV/m RMS. The most intense events predict source electric field amplitudes in excess of 1 V/m. Such wave amplitudes are rarely observed.

Figure 6 shows an example of wave emissions with >1 V/m electric field amplitude in the 300 Hz–16 kHz frequency band in the downward current region, which we define as a source region candidate. The observations in Fig. 6 are not from the vertex of an observed VLF saucer. We assume that a satellite must pass over a source region at a higher (or lower) altitude to observe a VLF saucer so a satellite passing through the source region will not detect the remote signature (VLF saucer). We identify source region candidates from peak wave electric field amplitudes (>1 V/m following the argument in the above paragraph) combined with intense, energetic antiearthward electron fluxes. A distinguishing characteristic of the candidate source regions is that intense whistler emissions co-exist with large-amplitude electron phase-space holes as seen in the perpendicular signal.

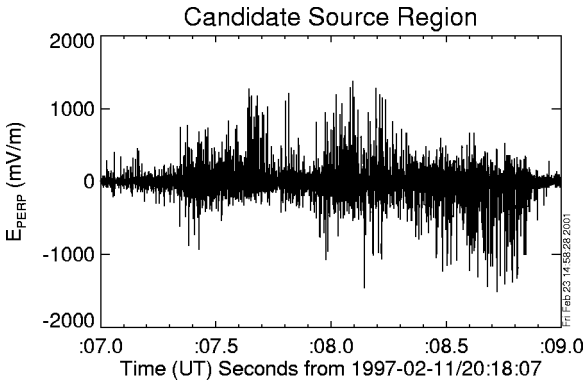

FIG. 6. The perpendicular (to B) electric field waveform seen with up-going energetic electron fluxes. The parallel signals (not shown) are saturated. The above waveform has intense (~200 mV/m) RMS power consisting of mixture of quasielectrostatic whistler waves and solitary structures interpreted as electron phase-space holes. The region is ~8 km in latitude.

Several (~10) such source region candidates were identified in a separate and much broader search for electron phase-space holes,[16] so the number of candidate source regions does not correspond to 100 VLF saucer identifications. In each case, the peak amplitudes were dominated by electron phase-space holes. Observation of source region candidates suggest a direct association between electron phase-space holes and whistler waves.

IV. GENERAL CHARACTERISTICS

A 100-event study was performed with the goal of determining general characteristics of VLF saucers. The events were the first one hundred selected by eye through examination of omni-directional VLF electric field power-frequency-time spectrograms (see Fig. 3). We were unable to develop a computer algorithm that made a reliable and unbiased identification of VLF saucers from the wave data. The orbits are from the 1997 Northern winter, a very active period. To be detectable by eye, the events had to have a frequency dispersive signature. Once selected, the characteristics of the electron distribution, the field-aligned currents, the dc electric field, magnetic field, and the plasma density were determined. The distance to the source region also was estimated [Eq. (4)].

Table I displays the association of VLF saucers with electron fluxes. Of the 100 events, 85 had a detectable downward current (magnitude >0.1 $\mu\mathrm{A/m}^2$) in the 10 eV to 30

TABLE I. Summary of VLF saucer survey.

Total number of events	Events with downward current	Events with upward current	Current <0.1 μA/m^2 in magnitude
100	85	7	8

keV electron fluxes, seven had a detectable upward current, and eight had no detectable current (magnitude <0.1 μA/m^2). All of the seven upward current events were at the edge of an ''inverted-V'' event and had intense, energetic, field-aligned electron fluxes that are known as edge precipitation.[22] Of the eight events that had no detectable current (magnitude <0.1 μA/m^2), 6 had very low electron fluxes, $<10^7$ (cm^2 s ster) in all energy channels >10 eV, and two had intense fluxes but no current. An immediate result of the study is the strong association of VLF saucers with >10 eV up-going electron fluxes, conclusively affirming the models put forth by Lonnqvist *et al.*[14] and James[9] that the VLF saucer energy source is primarily from up-going electron beams.

Of the 85 events in the downward current region, 67 of the events had broadband electrostatic noise (BEN) with spectral power density of 10^{-8} (V/m)^2/Hz or greater at or near the vertex (Table II). Of those 67 events, 37 had waveform captures. Electron phase-space holes were identified in all 37 of the waveform captures, strongly suggesting that all, or almost all of the 67 events with ''strong'' BEN were associated with electron phase-space holes. Of the remaining 18 downward current region events, 13 had BEN between 10^{-10} (V/m)^2/Hz and 10^{-8} (V/m)^2/Hz, which we shall call ''weak'' BEN. Of these events, three had waveform captures one of which had no detectable electron phase space holes and two had weak, sparse events. Of the five events that had no detectable BEN, two had waveform captures, both of which had no discernible electron phase-space holes.

From these results, we conclude that VLF saucers in the downward current region have a surprisingly strong association, $>79\%$ or 67 of 85 events, with electron phase-space holes. This strong association suggest a common energy source and, perhaps, that the electron phase-space holes as well as the whistlers and may come from the VLF saucer source region.

The VLF saucers that have electron phase-space holes at their vertex typically had stronger currents and significantly higher energies than the 18 events with weak or no BEN (Table II). The currents in Table II are the average of the peak current for each of the events as measured from the electron fluxes. The electron energies are averages of the characteristic energies of individual events. The characteristic energy is the integrated electron energy flux divided by the integrated electron number flux. There are several interpretations of this finding. It may be possible that the electron phase-space holes are produced in only the more intense events. Alternatively, the spacecraft may have ''missed'' the flux tube of the 18 events with no electron phase-space holes due to longitudinal displacement of the spacecraft.

TABLE II. BEN amplitude of the downward current region events.

Downward current region events	BEN$>10^{-8}$ (V/m)^{2}Hz	10^{-8} (V/m)^{2}Hz $>$BEN$>10^{-10}$ (V/m)^2/Hz	No detectable BEN
85	67	13	5
Current	3.1 μA/m^2	2.0 μA/m^2	
Electron energy	237 eV	88 eV	

TABLE III. Source distance of downward current region events.

Downward current region events	Source <300 km from spacecraft	Source>300 km from spacecraft
85	42	43
Current	2.84 μA/m^2	2.87 μA/m^2
Electron energy	172 eV	238 eV
Events with detectable electron phase-space holes	33	34

Interestingly, there was no significant variation in the current, electron energy, or occurrence of electron phase-space holes with the distance from the source (Table III). The source distances were broadly distributed from $\sim$10 km to $\sim$2000 km with the majority lying between 100 km and 500 km. The spectral signature of nearby source regions are difficult to distinguish from that of electron phase-space holes whereas the source distances >500 km are inaccurately determined. The median distance (300 km) may be a consequence of the identification process. In compiling Table III, the source distance for each event is the nearest if there were multiple sources. This finding suggests that electron phase-space holes may be long lived, often traveling more than 300 km. We caution that the distance calculations assumed a homogenous plasma.

V. DISCUSSION AND CONCLUSIONS

Earlier studies put forth evidence that VLF saucers are mostly in the downward current region, drawing their energy from up-going electron fluxes. The FAST instruments have continuous viewing of the field-aligned electron fluxes, independent of spin phase. This feature brings certainty to the energy source of VLF saucer events; 85 of 100 events were associated with up-going electron fluxes. Thus, FAST observations have provided definitive evidence that the VLF saucer source flux tubes most often have up-going, energetic (>10 eV), field-aligned electron fluxes. Interestingly, 7 of the 100 events were seen in the upward current region. These events all had highly field-aligned electron fluxes that originated from a cold (<10 eV) source. Such fluxes are often seen at the edges of arcs.[22]

Of the 85 events in the downward current region, the up-going electron fluxes are almost always surrounded by a diverging electric field structure which indicates acceleration by parallel electric fields on the flux tube below the spacecraft. This conclusion contains a subjective element; the diverging electric fields were identified by eye and no rigorous

criteria for ''diverging electric fields'' has been established. Such an effort is beyond the scope of this article. Nonetheless, the observations are suggestive of an association of VLF saucers and parallel electric fields in the downward current region.

The correlation between the VLF saucer source flux tube and diverging electric field structures is somewhat expected. Parallel electric fields have been identified as the primary energy source of up-going electrons[2,3] and VLF saucers were previous associated with up-going electrons. The intense, highly confined source of the VLF saucer emissions, however, suggests that it is very near to a region where the electrons are accelerated. It is possible then, that the parallel electric field is also highly confined. Thus, the source region may be very near, if not within, the region of parallel electric fields. The emerging fluxes not only acquire a strong antiearthward drift velocity, but also show evidence of strong wave-particle interactions which results in substantial parallel heating.[2] Thus the wave-particle interactions in the VLF saucer source may be important in understanding parallel electric fields in the downward current region.

The sizes of individual VLF saucer source regions inferred from the FAST data are in general agreement with those reported by James[9] who found that the source sizes are less than 10 km in altitude and ~0.5 km in latitude. The ISIS 2 satellite had active sounding which allowed for an estimate of the plasma density along the ray paths. Only the *in situ* density is available from FAST, so the ISIS 2 estimates on the sizes (and ranges) of far-away sources (>50 km) have better accuracy. FAST, however, is able to resolve nearby source regions, so as close as ~10 km and the size estimates of these nearby source regions also were consistent with the findings of James.[9] One nearby source, however, was determined to have a scales size along $\boldsymbol{B}$ of ~1 km (see discussion of Fig. 4). Such a size is roughly 10 to 100 Debye lengths, indicating an extremely fast and possible nonlinear growth process.

Close examination of the high-resolution observations reveal that the VLF saucer source regions may be confined in longitude as well. An accurate determination of the extent in longitude requires resolving the bandwidth near the vertex of an event. The VLF saucer vertices, however, often have broadband electrostatic noise due to electron phase-space holes, which increase the uncertainty of the longitudinal extent. In several examples in which an estimate could be made, the longitudinal size was found to be less than ~25 km. These findings suggest that some of the individual VLF saucer source regions are three-dimensionally confined.

The majority of VLF-saucer events display complex, multiple-arm structure that indicates several distinct, three-dimensionally confined source regions are distributed over a $O(10)$ km region in latitude, but may have greater separation (up to 1000 km) in altitude. The multiple arm structure in Fig. 3, for example, shows more that eight individual point sources. One of the most important unresolved questions is how to interpret the sources that are separated in altitude. Do they reside on the same flux tube or are they on adjacent flux tubes that are separated in latitude and/or longitude? Under the latter interpretation, there is only one source region on a flux tube. This question is difficult to answer as it requires a credible density model and accurate ray tracing.

The fact that most VLF saucer events had electron fluxes at their vertex indicates that the downward current system is sheet-like in longitude. If the downward currents were highly structured, one would expect more observations of VLF saucers with no detectable current and/or no apparent electron fluxes than the survey indicates. It is possible, however, that the electron fluxes measured at the vertex are not directly related to the observed saucer; the electron fluxes responsible for the whistler wave growth may have been longitudinally offset from the spacecraft's path. On the other hand, the vertices of the observed saucers were often consistent with the local lower hybrid frequency, so the longitudinal offsets were, in general, small. The observations suggest that multiple source regions, each of which is three-dimensionally confined to a small size, have dense coverage in longitude.

The intensities of whistler emissions of VLF saucers, when de-convolved to a small source size, indicate electric field amplitudes of $\boldsymbol{O}(1)$ V/m for strong events. Such wave amplitudes are rare, and when observed, are therefore identified as source region candidates. A common characteristic of the source region candidates is the combination of intense whistler emissions and electron phase-space holes (Fig. 6), suggesting a connection between the two phenomena.

The strong correlation between VLF saucers and electron phase space holes[6] may reveal properties of the whistler wave growth process in the VLF saucer source region. The data imply that the whistler emission from the VLF saucers and electron phase-space holes share a common energy source: the accelerated, field-aligned electron fluxes. One can take this idea one step further and consider if the whistler waves and the electron phase-space holes interact during the growth process. The small source size, large-amplitude wave electric fields, and rapid growth rate support such a nonlinear scenario. If the electron phase-space holes emerge from the same source region they also must undergo rapid growth.

The interaction between whistler waves and electron phase-space holes has some theoretical support. Numerical simulations of electron phase-space holes, generated with bidirectional electron beams as an initial condition, predict whistler emission during the growth and evolution of electron phase-space holes.[23–25] In the early stages in numerical simulations, 1D electron phase-space holes emerge and subsequently break up into 2D and 3D structures emitting whistler waves during the process. The whistler wave emissions intensify between ~100 $(1/\omega_{pe})$ to ~1000 $(1/\omega_{pe})$, with $\omega_{pe} \sim 10^5$ s^{-1} in the examples presented in this paper). Since electron phase-space holes have velocities of ~1000 km/s,[16] the break-up process must take place in a ~1 km to ~10 km region along $\boldsymbol{B}$.

The interaction between whistler waves and electron phase-space holes also has been investigated analytically. Newman and Goldman[26] and Newman *et al.*[27] predict a transverse instability in 1D electron phase-space holes which emit waves below the bounce frequency of the trapped electrons (typically ~1/3 ω_{pe}). These emissions propagate as whistler waves as they emerge from the source region. Vetoulis and Oppenheim[28] model a kinetic instability which

result in transverse wave emission at or above the bounce frequency. The observations, the numerical simulations, and the analytical work together suggest a physical connection between the VLF saucers and electron phase-space holes.

[1]C. W. Carlson, R. Pfaff, and J. G. Watzin, Geophys. Res. Lett. **25**, 2013 (1998).
[2]C. W. Carlson, J. P. McFadden, R. E. Ergun, M. Temerin, W. Peria, F. S. Mozer, D. M. Klumpar, E. G. Shelly, W. K. Peterson, E. Moebius, R. Elphic, R. Strangeway, C. Cattell, and R. Pfaff, Geophys. Res. Lett. **25**, 2017 (1998).
[3]R. E. Ergun, C. W. Carlson, J. P. McFadden, F. S. Mozer, G. T. Delory, W. Peria, C. C. Chaston, M. Temerin, R. Elphic, R. Strangeway, R. Pfaff, C. A. Cattell, D. Klumpar, E. Shelley, W. Peterson, E. Moebius, and L. Kistler, Geophys. Res. Lett. **25**, 2025 (1998).
[4]R. E. Ergun, C. W. Carlson, J. P. McFadden, F. S. Mozer, Y.-J. Su, L. Andersson, D. L. Newman, M. V. Goldman, and R. J. Strangeway, Phys. Rev. Lett. **87**, 045003 (2001).
[5]L. Andersson, R. E. Ergun, D. Newman, J. P. McFadden, C. W. Carlson, and Y.-J. Su, Phys. Plasma (submitted).
[6]R. E. Ergun, M. V. Goldman, D. L. Newman, C. W. Carlson, J. P. McFadden, and R. J. Strangeway, Geophys. Res. Lett. **28**, 3805 (2001).
[7]R. L. Smith, L. Kimura, J. Vigneron, and J. Katsufrakis, J. Geophys. Res. **71**, 1925 (1966).
[8]D. A. Gurnett, J. Geophys. Res. **71**, 5599 (1966).
[9]H. G. James, J. Geophys. Res. **81**, 501 (1976).
[10]R. L. Smith, Nature (London) **224**, 351 (1969).
[11]S. R. Mosier and D. A. Gurnett, J. Geophys. Res. **74**, 5675 (1969).
[12]M. Temerin, J. Geophys. Res. **84**, 6691 (1979).
[13]M. Temerin, C. Cattell, R. Lysak, M. Hudson, R. B. Torbert, F. S. Mozer, R. D. Sharp, and P. M. Kintner, J. Geophys. Res. B **86**, 11 278 (1981).
[14]H. Lonnqvist, M. Andre, L. Matson, A. Bahnsen, L. G. Blomberg, and R. E. Erlandson, J. Geophys. Res., [Oceans] **98**, 13 565 (1993).
[15]D. A. Gurnett and L. A. Frank, J. Geophys. Res. **77**, 172 (1972).
[16]R. E. Ergun, C. W. Carlson, J. P. McFadden, F. S. Mozer, G. T. Delory, W. Peria, C. C. Chaston, M. Temerin, R. Elphic, R. Strangeway, R. Pfaff, C. A. Cattell, D. Klumpar, E. Shelly, W. Peterson, E. Moebius, and L. Kistler, Geophys. Res. Lett. **25**, 2041 (1998).
[17]R. E. Ergun, C. W. Carlson, J. P. McFadden, F. S. Mozer, L. Muschietti, I. Roth, and R. J. Strangeway, Phys. Rev. Lett. **81**, 826 (1998).
[18]R. L. Tokar and S. P. Gary, Geophys. Res. Lett. **11**, 1180 (1984).
[19]C. W. Carlson, J. P. McFadden, P. Turin, D. W. Curtis, and A. Magoncelli, Space Sci. Rev. **98**, 33 (2001).
[20]R. E. Ergun, C. W. Carlson, F. S. Mozer, G. T. Delory, M. Temerin, J. P. McFadden, D. Pankow, R. Abiad, P. Harvey, R. Wilkes, H. Primbsch, R. Elphic, R. Strangeway, R. Pfaff, and C. A. Cattell, Space Sci. Rev. **98**, 67 (2001).
[21]R. C. Elphic, J. D. Means, R. C. Snare, R. J. Strangeway, L. Kepko, and R. E. Ergun, Space Sci. Rev. **98**, 151 (2001).
[22]J. P. McFadden, C. W. Carlson, and M. H. Boehm, J. Geophys. Res., [Space Phys.] **91**, 1723 (1986).
[23]M. V. Goldman, M. M. Oppenheim, and D. L. Newman, in *Physics of Space Plasmas 15*, edited by T. Chang and J. R. Jasperse (Cambridge University Press, Cambridge, MA, 1998).
[24]M. V. Goldman, M. M. Oppenheim, and D. L. Newman, Geophys. Res. Lett. **26**, 1821 (1999).
[25]M. M. Oppenheim, D. L. Newman, and M. V. Goldman, Phys. Rev. Lett. **83**, 2344 (1999).
[26]D. L. Newman and M. V. Goldman, Phys. Scr. **T89**, 76 (2001).
[27]D. L. Newman, M. V. Goldman, M. Spector, and F. Perez, Phys. Rev. Lett. **86**, 1239 (2001).
[28]G. Vetoulis and O. Meers, Phys. Rev. Lett. **86**, 1235 (2001).